

# Stability of Q-balls and Catastrophe

Nobuyuki Sakai\*

*Department of Education, Yamagata University, Yamagata 990-8560, Japan*

Misao Sasaki†

*Yukawa Institute for Theoretical Physics,  
Kyoto University, Kyoto 990-8502, Japan*

(Dated: May 27, 2019)

## Abstract

We propose a practical method for analyzing stability of Q-balls for the whole parameter space, which includes the intermediate region between the thin-wall limit and thick-wall limit as well as Q-bubbles (Q-balls in false vacuum), using the catastrophe theory. We apply our method to the two concrete models,  $V_3 = m^2\phi^2/2 - \mu\phi^3 + \lambda\phi^4$  and  $V_4 = m^2\phi^2/2 - \lambda\phi^4 + \phi^6/M^2$ . We find that  $V_3$  and  $V_4$  Models fall into *fold catastrophe* and *cusp catastrophe*, respectively, and their stability structures are quite different from each other.

PACS numbers: 03.75.Lm

---

\*Electronic address: nsakai@e.yamagata-u.ac.jp

†Electronic address: misao@yukawa.kyoto-u.ac.jp

Q-balls [1], a kind of non-topological solitons [2], appear in a large family of field theories with global U(1) (or more) symmetry, and could play an important role in cosmology. For example, the Minimal Supersymmetric Standard Model may contain baryonic Q-balls, which could be responsible for baryon asymmetry [3] and dark matter [4].

The stability of Q-balls has been studied in the literature. Coleman argued that Q-balls are absolutely stable if the charge  $Q$  is sufficiently large, using the thin-wall approximation [1]. Kusenko showed that Q-balls with small  $Q$  are also stable for the potential

$$V_3(\phi) = \frac{m^2}{2}\phi^2 - \mu\phi^3 + \lambda\phi^4 \quad \text{with} \quad m^2, \mu, \lambda > 0, \quad (1)$$

using the thick-wall approximation [5]. Here the thick-wall limit is defined by the limit of  $\omega^2 \rightarrow m^2$ , where  $\omega$  is the angular velocity of phase rotation. Multamaki and Vilja found that in the thick-wall limit the stability depends on the form of the potential [6]. Paccetti Correia and Schmidt showed a useful theorem which applies to any equilibrium Q-balls [7]: their stability is determined by the sign of  $(\omega/Q)dQ/d\omega$ .

It is usually assumed that the potential has an absolute minimum at  $\phi = 0$ . If  $V(0)$  is a local minimum and the absolute minimum is located at  $\phi \neq 0$ , true vacuum bubbles may appear [8]. If  $Q = 0$ , vacuum bubbles are unstable: either expanding or contracting. Kusenko [9] and Paccetti Correia and Schmidt [7] showed, however, that there are stable bubbles if  $Q \neq 0$ . They called those solutions “Q-balls in the false vacuum”. Hereafter we simply call them “Q-bubbles”.

The standard method for analyzing stability is to take the second variation of the total energy (given by Eq.(9) below) and evaluate its sign. However, this calculation can be executed analytically only for some limited cases; in general the eigenvalue problem should be solved numerically, as Axenides *et al.* did [10]. In this paper, we propose an easy and practical method for analyzing stability with the help of the catastrophe theory. The basic idea of the catastrophe theory is described in Appendix. As we shall show below, once we find *behavior variable(s)*, *control parameter(s)* and a *potential* in the Q-ball system, it is easy to understand the stability structure of Q-balls for the whole parameter space including the intermediate region between the thin-wall limit and thick-wall limit as well as Q-bubbles.

Consider an SO(2)-symmetric scalar field, whose action is given by

$$\mathcal{S} = \int d^4x \left[ -\frac{1}{2}\eta^{\mu\nu} \{ \partial_\mu \phi_1 \partial_\nu \phi_1 + \partial_\mu \phi_2 \partial_\nu \phi_2 \} - V(\phi) \right], \quad \text{with} \quad \phi \equiv \sqrt{\phi_1^2 + \phi_2^2}. \quad (2)$$

We consider spherically symmetric configurations of the field. Assuming homogeneous phase rotation,

$$(\phi_1, \phi_2) = \phi(r)(\cos \omega t, \sin \omega t), \quad (3)$$

the field equation becomes

$$\frac{d^2\phi}{dr^2} = -\frac{2}{r}\frac{d\phi}{dr} - \omega^2\phi + \frac{dV}{d\phi}. \quad (4)$$

This is equivalent to the field equation for a single static scalar field with the potential  $V_\omega \equiv V - \omega^2\phi^2/2$ . Due to the symmetry there is a conserved charge,

$$Q \equiv \int d^3x (\phi_1 \partial_t \phi_2 - \phi_2 \partial_t \phi_1) = \omega I, \quad \text{where} \quad I \equiv \int d^3x \phi^2. \quad (5)$$

Monotonically decreasing solutions  $\phi(r)$  with the boundary conditions,

$$\frac{d\phi}{dr}(0) = 0, \quad \phi(\infty) = 0, \quad (6)$$

exist if  $\min(V_\omega) < V(0)$  and  $d^2V_\omega/d\phi^2(0) > 0$ , which is equivalent to

$$\omega_{\min}^2 < \omega^2 < m^2 \quad \text{with} \quad \omega_{\min}^2 \equiv \min\left(\frac{2V}{\phi^2}\right), \quad m^2 \equiv \frac{d^2V}{d\phi^2}(0), \quad (7)$$

where we have put  $V(0) = 0$  without loss of generality. The two limits  $\omega^2 \rightarrow \omega_{\min}^2$  and  $\omega^2 \rightarrow m^2$  correspond to the thin-wall limit and the thick-wall limit, respectively. The condition  $\omega_{\min}^2 < m^2$  is not so restrictive because it is satisfied if the potential has the form,

$$V = \frac{m^2}{2}\phi^2 - \lambda\phi^n + O(\phi^{n+1}) \quad \text{with} \quad m^2 > 0, \quad \lambda > 0, \quad n \geq 3. \quad (8)$$

The total energy of the system for equilibrium solutions is given by

$$E = \frac{Q^2}{2I} + \int d^3x \left\{ \frac{1}{2} \left( \frac{d\phi}{dr} \right)^2 + V \right\}. \quad (9)$$

Note that the variation of  $E$  under fixed  $Q$ ,  $\delta E/\delta\phi|_Q = 0$ , reproduces the field equation (4).

Let us discuss how we apply the catastrophe theory to the present Q-ball system. The catastrophe theory is briefly described in Appendix. An essential point is to choose *behavior variable(s)*, *control parameter(s)* and a *potential* in the Q-ball system appropriately. For a given potential  $V(\phi)$  and charge  $Q$ , we consider a one-parameter family of perturbed field configurations  $\phi_\omega(r)$  near the equilibrium solution  $\phi(r)$ . The one-parameter family is chosen to satisfy  $I[\phi_\omega] = Q/\omega$ . Then the energy is regarded as a function of  $\omega$ ,  $E(\omega) \equiv E[\phi_\omega]$ .

Because  $dE/d\omega = (\delta E/\delta\phi_\omega)d\phi_\omega/d\omega = 0$  when  $\phi_\omega$  is an equilibrium solution,  $\omega$  may be regarded as a *behavior variable* and  $E$  as the *potential*. On the other hand, the charge  $Q$  and the model parameter(s) of  $V(\phi)$  can be given by hand, and therefore should be regarded as *control parameters*. We denote the model parameter(s) by  $P_i$  ( $i = 1, 2, \dots$ ). Then we analyze the stability of Q-balls as follows.

- Solve the field equation (4) with the boundary condition (6) numerically to obtain equilibrium solutions  $\phi(r)$  for various values of  $\omega$  and model parameter(s)  $P_i$ .
- Calculate  $Q$  by (5) for each solution to obtain the *equilibrium space*  $M = \{(\omega, P_i, Q)\}$ . We denote the equation that determines  $M$  by  $f(\omega, P_i, Q) = 0$ .
- Find folding points where  $\partial P_i/\partial\omega = 0$  or  $\partial Q/\partial\omega = 0$  in  $M$ , which are identical to the stability-change points,  $\Sigma = \{(\omega, P_i, Q) \mid \partial f/\partial\omega = 0, f = 0\}$ .
- Calculate the energy  $E$  by (9) for equilibrium solutions around a certain point in  $\Sigma$  to find whether the point is a local maximum or a local minimum. Then we find the stability structure for the whole  $M$ .

Now, using the method devised above, we investigate the stability of equilibrium Q-balls. Because in the thick-wall limit the stability depends on whether  $n = 3$  or  $n \geq 4$  in (8) [6, 7],

we consider two specific models. One is given by (1), which we call  $V_3$  Model, and the other is given by

$$V_4(\phi) = \frac{m^2}{2}\phi^2 - \lambda\phi^4 + \frac{\phi^6}{M^2} \quad \text{with} \quad m^2, \lambda, M^2 > 0, \quad (10)$$

which we call  $V_4$  Model. For  $V_3$  Model, rescaling the quantities as

$$\tilde{t} \equiv \frac{\mu}{\sqrt{\lambda}}t, \quad \tilde{r} \equiv \frac{\mu}{\sqrt{\lambda}}r, \quad \tilde{\phi} \equiv \frac{\lambda}{\mu}\phi, \quad \tilde{V}_3 \equiv \frac{\lambda^3}{\mu^4}V_3, \quad \tilde{m} \equiv \frac{\sqrt{\lambda}}{\mu}m, \quad \tilde{\omega} \equiv \frac{\sqrt{\lambda}}{\mu}\omega, \quad (11)$$

the field equation (4), the potential (1), the charge (5) and the energy (9) are rewritten as

$$\frac{d^2\tilde{\phi}}{d\tilde{r}^2} = -\frac{2}{\tilde{r}}\frac{d\tilde{\phi}}{d\tilde{r}} - \tilde{\omega}^2\tilde{\phi} + \frac{d\tilde{V}_3}{d\tilde{\phi}}, \quad \tilde{V}_3 = \frac{\tilde{m}^2}{2}\tilde{\phi}^2 - \tilde{\phi}^3 + \tilde{\phi}^4, \quad \tilde{E} = \frac{\lambda^{\frac{3}{2}}}{M}E, \quad \tilde{Q} = \lambda Q. \quad (12)$$

Similarly, for  $V_4$  Model, rescaling the quantities as

$$\tilde{t} \equiv \lambda Mt, \quad \tilde{r} \equiv \lambda Mr, \quad \tilde{\phi} \equiv \frac{\phi}{\sqrt{\lambda M}}, \quad \tilde{V}_4 \equiv \frac{V_4}{\lambda^3 M^4}, \quad \tilde{m} \equiv \frac{m}{\lambda M}, \quad \tilde{\omega} \equiv \frac{\omega}{\lambda M}, \quad (13)$$

the field equation (4), the potential (10), the charge (5) and the energy (9) are rewritten as

$$\frac{d^2\tilde{\phi}}{d\tilde{r}^2} = -\frac{2}{\tilde{r}}\frac{d\tilde{\phi}}{d\tilde{r}} - \tilde{\omega}^2\tilde{\phi} + \frac{d\tilde{V}_4}{d\tilde{\phi}}, \quad \tilde{V}_4 = \frac{\tilde{m}^2}{2}\tilde{\phi}^2 - \tilde{\phi}^4 + \tilde{\phi}^6, \quad \tilde{E} = \frac{E}{M}, \quad \tilde{Q} = \frac{Q}{\lambda}. \quad (14)$$

In both models the system is regarded as a mechanical system with the *behavior variable*  $\tilde{\omega}$ , the *control parameters*  $\tilde{m}^2$  and  $\tilde{Q}$ , and the *potential*  $\tilde{E}(\tilde{\omega}; \tilde{m}^2, \tilde{Q})$ . Because  $\tilde{\omega}_{\min}^2 = \tilde{m}^2 - 1/2$ , the existing condition (7) reduces to

$$0 < \tilde{m}^2 - \tilde{\omega}^2 < \frac{1}{2}. \quad (15)$$

The thin-wall and thick-wall limits correspond to  $\tilde{m}^2 - \tilde{\omega}^2 \rightarrow 1/2$  and  $\tilde{m}^2 - \tilde{\omega}^2 \rightarrow 0$ , respectively. The condition for ordinary Q-balls,  $\tilde{\omega}_{\min}^2 \geq 0$ , reduces to  $\tilde{m}^2 \geq 1/2$ , while that for Q-bubbles,  $\tilde{\omega}_{\min}^2 < 0$ , to  $\tilde{m}^2 < 1/2$ .

Figures 1 and 2 show the structures of the *equilibrium spaces*,  $M = \{(\tilde{\omega}, \tilde{m}^2, \tilde{Q})\}$ , and their catastrophe map,  $\chi(M)$ , into the *control planes*,  $C = \{(\tilde{m}^2, \tilde{Q})\}$ , for  $V_3$  and  $V_4$  Models, respectively. We only show the results for  $\tilde{\omega} > 0$ ; the sign transformation  $\tilde{\omega} \rightarrow -\tilde{\omega}$  changes nothing but  $\tilde{Q} \rightarrow -\tilde{Q}$ . The dash-dotted lines in  $M$  denote stability-change points  $\Sigma$ . Because the equilibrium space alone does not tell us which lines, solid or dashed, represent stable solutions, we evaluate the energy  $\tilde{E}$  for several equilibrium solutions, as shown in Figs. 3 and 4. When there are double or triple values of  $\tilde{E}$  for a given set of the control parameters  $(\tilde{m}^2, \tilde{Q})$ , by energetics the solution with the lowest value of  $\tilde{E}$  should be stable and the others should be unstable. In Figs. 3 and 4, we also give a sketch of the *potential*  $E(\omega; \tilde{m}^2, \tilde{Q})$  near the equilibrium solutions. Once the stability for a given set of the parameters  $(\tilde{m}^2, \tilde{Q})$  is found, the stability for all the sets of parameters which may be reached continuously from that set without crossing  $\Sigma$  is the same. We therefore conclude that, in Figs. 1 and 2 as well as in Figs. 3 and 4, solid and dashed lines correspond to stable and unstable solutions, respectively.

According to the configurations of  $\chi(\Sigma)$  in the *control planes* in Figs. 1 and 2, we find that  $V_3$  Model falls into *fold catastrophe* while  $V_4$  Model falls into *cusp catastrophe*. In the

*control planes*, the numbers of stable and unstable solutions for each  $(\tilde{m}^2, \tilde{Q})$  are represented by N, S, U, SU and SUU (see the figure captions for their definitions). Thus we find the stability structures of the two models are very different from each other. They are found as follows.

### **$V_3$ Model**

- $\tilde{m}^2 \geq 1/2$ : All equilibrium solutions are stable.
- $\tilde{m}^2 < 1/2$  (Q-bubbles): For each  $\tilde{m}^2$  there is a maximum charge,  $\tilde{Q}_{\max}$ , above which equilibrium solutions do not exist. For  $\tilde{Q} < \tilde{Q}_{\max}$ , stable and unstable solutions coexists. It is interesting to note that stable Q-bubbles exist no matter how small  $\tilde{Q}$  is.

### **$V_4$ Model**

- $\tilde{m}^2 \geq 1/2$ : For each  $\tilde{m}^2$  there is a minimum charge,  $\tilde{Q}_{\min}$ , below which equilibrium solutions do not exist. For  $\tilde{Q} > \tilde{Q}_{\min}$ , stable and unstable solutions coexists.
- $\tilde{m}^2 < 1/2$  (Q-bubbles): For each  $\tilde{m}^2$  there is a maximum charge,  $\tilde{Q}_{\max}$ , as well as a minimum charge,  $\tilde{Q}_{\min}$ , where stable solutions do not exist if  $\tilde{Q} < \tilde{Q}_{\min}$  or  $\tilde{Q} > \tilde{Q}_{\max}$ . For  $\tilde{Q}_{\min} < \tilde{Q} < \tilde{Q}_{\max}$ , there are one stable and two unstable solutions.  
As  $\tilde{m}^2$  becomes smaller,  $\tilde{Q}_{\max}$  and  $\tilde{Q}_{\min}$  come close to each other, and finally merge at  $\tilde{m}^2 \approx 0.26$ , below which there is no stable solution.

The above results for the two models are consistent with the previous results for some special cases such as thin-wall limit, the thick-wall limit and bubbles with  $Q = 0$ .

Many years ago Maeda *et al.* utilized the catastrophe theory for studying the stability of exotic back-holes [11]. The present work indicates that the catastrophe theory is also a useful tool for studying solitons in field theory. In this work we have not taken gravity into account. However, gravity may play an important role in cosmological situations. Therefore it is worthwhile to consider the extension of our analysis to the case of gravitating solitons.

We thank H. Kodama, K. Maeda, K. Nakao, V. Rubakov, H. Shinkai, T. Tanaka and S. Yoshida for useful discussions. A part of this work was done while NS was visiting at Yukawa Institute for Theoretical Physics, which was supported by Center for Diversity and Universality in Physics (21COE) in Kyoto University. The numerical computations of this work were carried out at the Yukawa Institute Computer Facility. This work was supported in part by JSPS Grant-in-Aid for Scientific Research (B) No. 17340075, (A) No. 18204024 and (C) No. 18540248.

## **APPENDIX A: BASIC IDEA OF CATASTROPHE THEORY**

To illustrate the basic idea of the catastrophe theory [12], we consider a system with one *behavior variable*  $x$ , two *control parameters*  $p, q$  and a *potential*  $F(x; p, q)$ . An equilibrium point of  $x$  is determined by  $dF/dx = 0$  for each pair of  $(p, q)$ . The set of the control parameters,  $C \equiv (p, q)$ , spans a plane called the *control plane*, and the set of equilibrium points,

$$M \equiv \left\{ (x, p, q) \mid f(x, p, q) \equiv \frac{dF}{dx} = 0 \right\}, \quad (\text{A1})$$

is called the *equilibrium space*. Because equilibrium points are stable if  $\partial f/\partial x > 0$ , the boundary of stable and unstable equilibrium points are given by the curve,

$$\Sigma \equiv \left\{ (x, p, q) \mid \frac{\partial f}{\partial x} = 0, f = 0 \right\}. \quad (\text{A2})$$

The *catastrophe map* is defined as

$$\chi: M \rightarrow C, \quad (x, p, q) \rightarrow (p, q). \quad (\text{A3})$$

Depending on the properties of the image  $\chi(\Sigma)$ , mechanical systems with stability-change are classified into several catastrophe types.

If the *potential*  $F(x; p, q)$  is known, it is easy to find equilibrium points and their stability. However, even if we do not know the explicit form of  $F(x; p, q)$ , we can still find  $\Sigma$  by analyzing equilibrium points as follows.

The Taylor expansion of  $f(x, p, q)$  in the vicinity of a certain point  $P(x_0, p_0, q_0)$  in  $M$ , where  $f = 0$ , up to the first order yields

$$q = q(x, p) = q_0 - \left( \frac{\partial f}{\partial q} \right)^{-1} \left\{ \frac{\partial f}{\partial x} (x - x_0) + \frac{\partial f}{\partial p} (p - p_0) \right\}, \quad \text{if } \frac{\partial f}{\partial q} \neq 0. \quad (\text{A4})$$

Because  $\partial f/\partial x = 0$  in  $\Sigma$ , it follows from (A4) that  $\partial q/\partial x = 0$  in  $\Sigma$ . Similarly, unless  $\partial f/\partial x = 0$ ,  $\partial p/\partial x = 0$  in  $\Sigma$ . Therefore, surveying the points with  $\partial p/\partial x = 0$  or  $\partial q/\partial x = 0$  in the *equilibrium space*  $M$ , we can obtain the set of stability-change points  $\Sigma$ .

- 
- [1] S. Coleman, Nucl. Phys. **B262**, 263 (1985).
  - [2] For a review of non-topological solitons, see, T. Lee and Y. Pang, Phys. Rep. **221**, 251 (1985).
  - [3] K. Enqvist and J. McDonald, Phys. Lett. B **425**, 309 (1998).
  - [4] A. Kusenko and M. Shaposhnikov, Phys. Lett. B **418**, 46 (1998).
  - [5] A. Kusenko, Phys. Lett. B **404**, 285 (1997).
  - [6] T. Multamaki and I. Vilja, Nucl. Phys. B **574**, 130 (2000).
  - [7] F. Paccetti Correia and M. G. Schmidt, Eur. Phys. J. **C21**, 181 (2001).
  - [8] S. Coleman, Phys. Rev. D **15**, 2929 (2000).
  - [9] A. Kusenko, Phys. Lett. B **406**, 26 (1997).
  - [10] M. Axenides, S. Komineas, L. Perivolaropoulos and M. Floratos, Phys. Rev. D **61**, 085006 (2000).
  - [11] K. Maeda, T. Tachizawa, T. Torii and T. Maki, Phys. Rev. Lett. **72**, 450 (1997); T. Torii, K. Maeda and T. Tachizawa, Phys. Rev. D **51**, 1510 (1995); T. Tachizawa, K. Maeda and T. Torii, *ibid.* **51**, 4054 (1995); T. Torii, K. Maeda and T. Tachizawa, *ibid.* **52**, R4272 (1995); K. Maeda, J. Korean Phys. Soc. **28**, S468 (1995).
  - [12] For a review of the catastrophe theory, see, e.g., T. Poston and I.N. Stewart, *Catastrophe Theory and Its Application*, Pitman (1978).

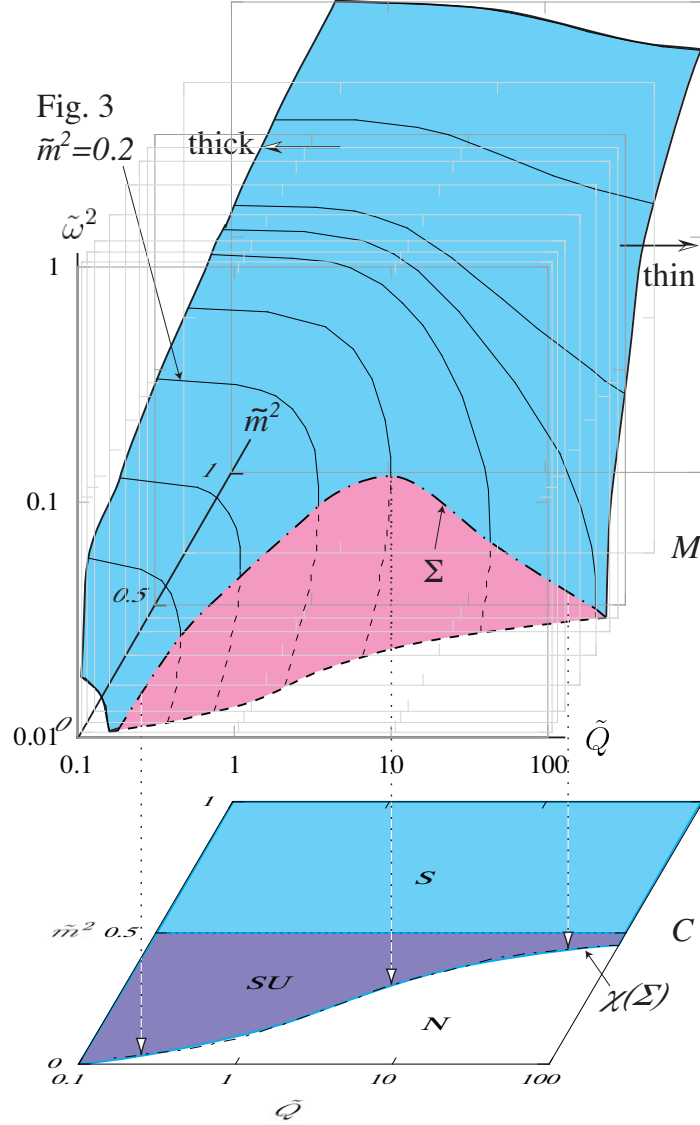


FIG. 1: Structures of the *equilibrium spaces*,  $M = \{(\tilde{\omega}, \tilde{m}^2, \tilde{Q})\}$ , and their catastrophe map,  $\chi(M)$ , into the *control planes*,  $C = \{(\tilde{m}^2, \tilde{Q})\}$ , for  $V_3$  Model. The dash-dotted lines in  $M$  denote stability-change points  $\Sigma$ , and the dash-dotted lines in  $C$  denote their catastrophe maps  $\chi(M)$ . Solid lines in  $M$  (on the light-cyan colored surface) and dashed lines (on the light-magenta colored surface) represent stable and unstable solutions, respectively. The arrows indicated by “thin” and “thick” show the thin-wall limit,  $\tilde{\omega}^2 \rightarrow \tilde{\omega}_{\min}^2 = \tilde{m}^2 - 1/2$ , and the thick-wall limit,  $\tilde{\omega}^2 \rightarrow \tilde{m}^2$ , respectively. In the regions denoted by  $S$ ,  $SU$  and  $N$  on  $C$ , there are one stable solution, one stable and one unstable solutions, and no equilibrium solution, respectively, for fixed  $(\tilde{m}^2, \tilde{Q})$ .

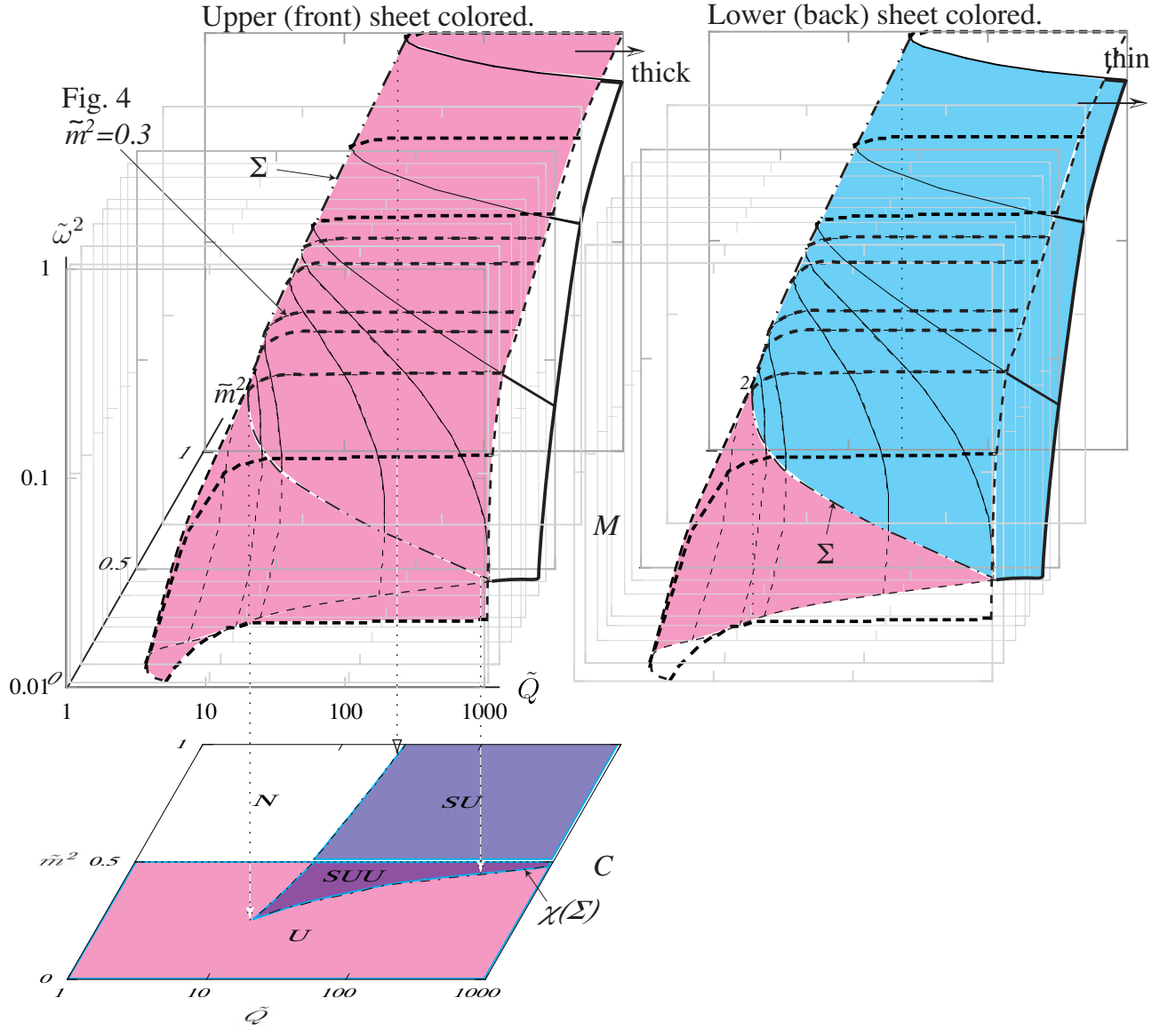


FIG. 2: The same as Fig. 1, but for  $V_4$  Model. Because the structure of  $M$  is complicated in this case, we show two pictures of  $M$ : The left one shows the upper (front) sheet of the equilibrium space, while the right one the lower (back) sheet. In the regions denoted by  $N$ ,  $U$ ,  $SU$  and  $SUU$  on  $C$ , there are no equilibrium solution, one unstable solution, one stable and one unstable solutions, and one stable and two unstable solutions, respectively, for fixed  $(\tilde{m}^2, \tilde{Q})$ .



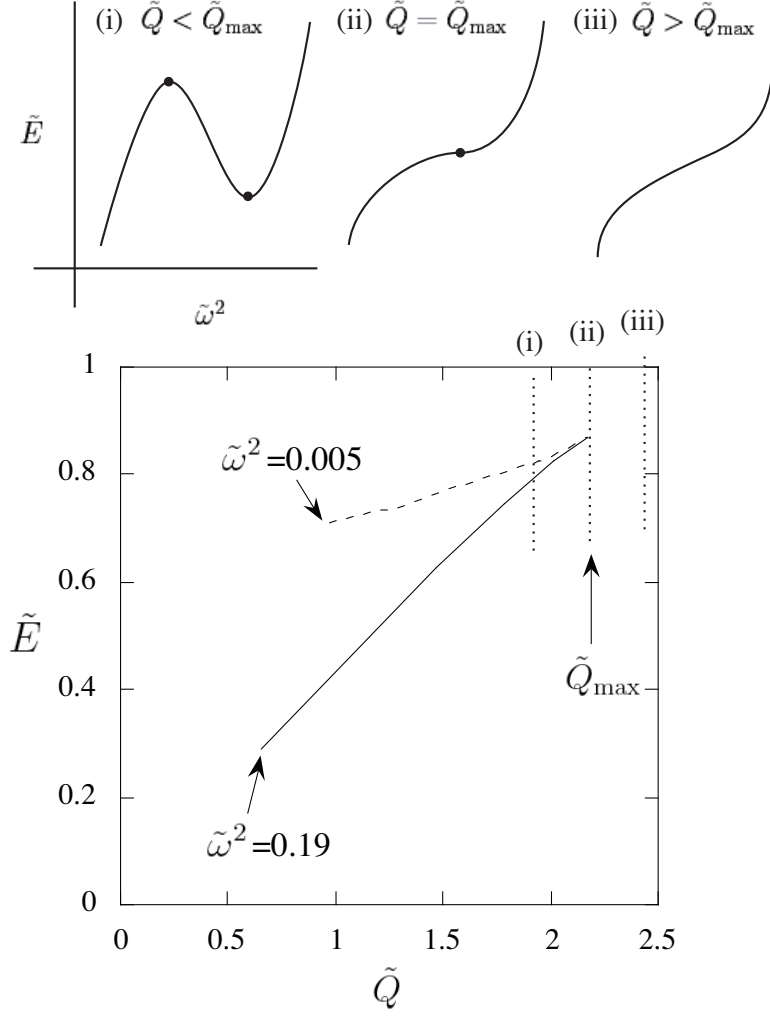


FIG. 3: A schematic picture of the *potential*  $E(\omega; \tilde{m}^2, \tilde{Q})$  of  $V_3$  Model with  $\tilde{m}^2 = 0.2$  near the equilibrium solutions, and the locus of equilibrium solutions on  $(\tilde{Q}, \tilde{E})$  plane. The solid and dashed lines represent stable and unstable solutions, respectively.

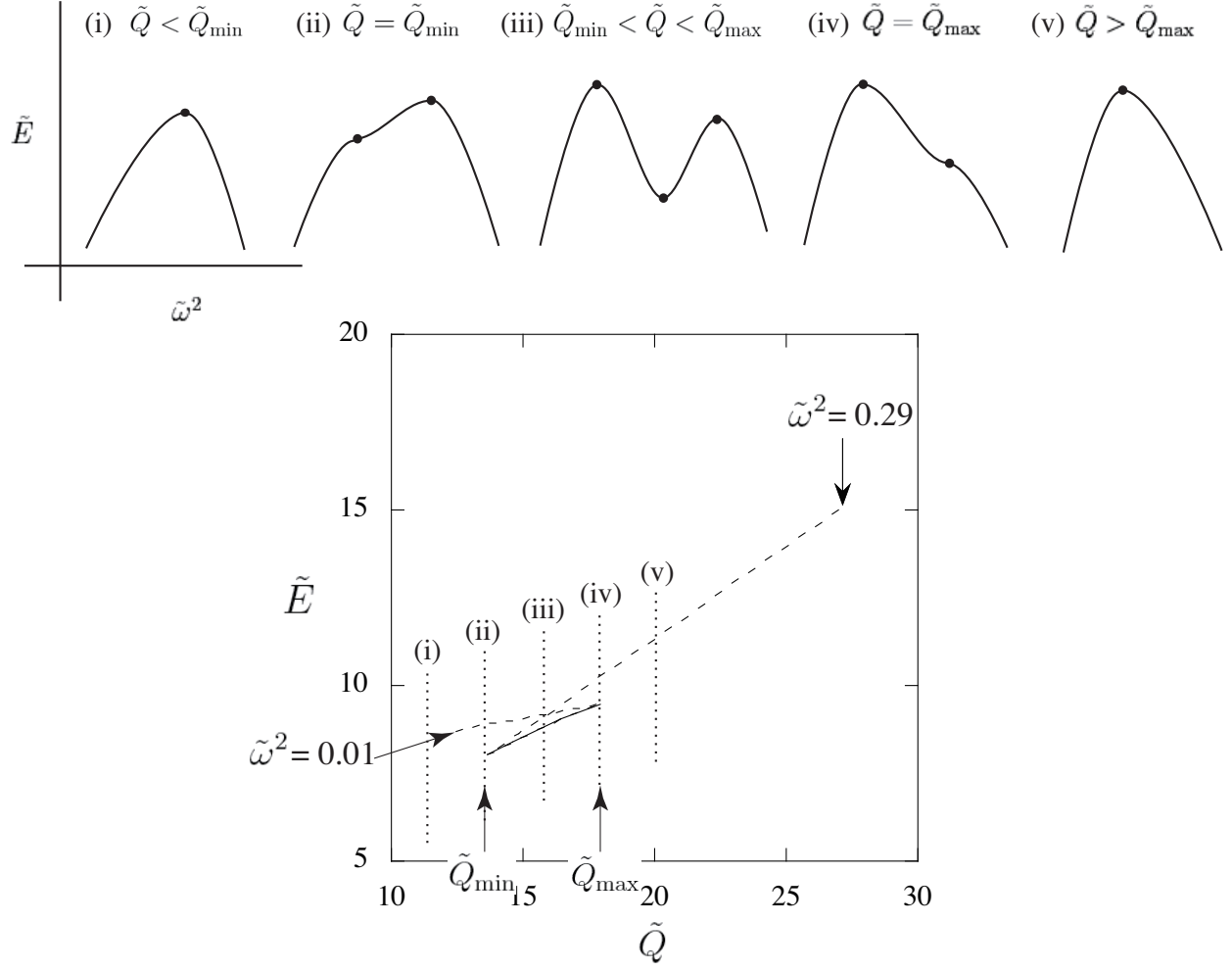


FIG. 4: The same as Fig. 3, but for  $V_4$  Model with  $\tilde{m}^2 = 0.3$ .